All-laser Fabrication of Metallic Nanoantenna with Planar Lens for Surface Plasmon Polaritons

S. V. Makarov[1, 2], **A. A. Ionin**[2], **S. I. Kudryashov**[2, 3], **and A. A. Kuchmizhak**[4]

[1]ITMO University, Kronverkskiy pr. 49, Saint-Petersburg, Russia
[2]P. N. Lebedev Physical Institute of the Russian Academy of Sciences
Leninskiy pr. 53, Moscow, Russia
[3]NRNU "MEPhI", Kashirskoe sh. 31, Moscow, Russia
[4]Institute of Automation and Control Processes
Far Eastern Branch, Russian Academy of Science, Vladivostok 690041, Russia

Abstract— We demonstrate new simple methods of all-laser fabrication of nanoantenna (nanojet) with an additional elements for coupling/focusing of surface plasmon-polaritons (SPPs). The first method is realized by using an aluminum (Al) plasmonic lens irradiated by a linearly polarized femtosecond laser pulse at fluences higher than the ablation threshold of aluminum. The resulting plasmonic lenses contain single nanojets in their centers owing to focusing of intense surface plasmon-polaritons and melt expulsion in the locally heated area. Such surface structure resembles a parabolic antenna, which has a receiver and focusing reflector. The second method is based on double-shot femtosecond laser nanoablation of thin supported metallic (Au) film. The first fs-laser pulse produces nanojet, standing on bump of microscale diameter. Irradiation by spatially shifted (on several microns) second laser pulse results in the bump removing, transition of nanojet into nanosphere and formation of concentric periodical semi-rings. Resulted surface structure represents nanoantenna (gold nanospere), surrounded by plasmonic lens, delivering more incident energy to the nanoantenna.

1. INTRODUCTION

Optical nanoantennas (ONAs), representing metal nanoparticles or nanorods of various shapes, demonstrate high localization and manipulation of optical radiation at nanoscale. Formation of such localized "hot spots" can significantly improve performance of molecular sensors [1] and solar cells [2]. For these applications, it is often necessary to fabricate sufficiently large ordered ONA arrays, which are now realized by a number of relatively expensive or time-consuming techniques. Hence, high-performance, low-cost techniques based on pulsed laser nanoablation of thin films to imprint various ONA types (nanojets [3–5], nanoholes [6, 7], and nanoparticles [8]), are needed to be developed. Preferences are given to femtosecond laser pulses, which initiate a multi-scale sequence of electrodynamic, thermal, and hydrodynamic processes, yielding inablation at timescales $\sim$ 1–10 ns. These processes are currently the subject of a broad fundamental research [9, 10]. Previously, laser-assisted fabrication of such nanoantennas on thin films was carried out with single-pulse irradiation; however, controllable fabrication of ONA arrays containing a central nanotip and an annular micropit was recently demonstrated via consecutive double-pulse irradiation of bulk Al surface [11, 12]. We demonstrate that capabilities of single-pulse nanostructuring techniques can be significantly expanded for advanced ONA fabrication, applying a second laser pulse. In this approach, the first pulse produces the primary nanostructure, while the second one imprints nearby an excited SPPs.

2. NANOANTENNA FABRICATION DUE TO FLASH-IMPRINT OF INTENSE SPP

In our experiments, 200-fs (FWHM), second-harmonic (515 nm) linearly-polarized pulses of an Yb-doped fiber laser with the maximum pulse energy of 4 μJ in the TEM00-mode ($M^2 \approx 1.05$) were focused by an aspherical lens (NA = 0.5) onto a sample surface (110-nm-thick Au film on a bulk Si substrate). The laser energy was varied by means of an output acousto-optical modulator and a reflective attenuator. The sample was arranged on a PC-controlled 3D-motorized micropositioning platform with a minimal translation step of 150 nm. The Au film was deposited onto the Si substrate by e-beam evaporation process (Ferrotec EV M-6) at a pressure of $5 \cdot 10^{-6}$ bar and constant deposition rate $\approx$ 4Å/s. To increase adhesion of the deposited material to the substrate, the latter was pre-cleaned with a built-in ion source (KRI EH200). The film thickness was preliminary measured, using a calibrated piezoelectric resonator (Sycon STC-2002) mounted inside the vacuum

chamber, and an atomic force microscope (AFM, NanoDST Pacific Nanotechnology). The resulting surface topology was characterized by scanning electron (SEM, JEOL 7001F) and the AFM microscopes.

According to numerous previous studies [3, 4, 9, 10], single fs-pulse impact leads to formation of two main features on a thin Au film: either a submicron through hole surrounded by a rim of solidified melt (high fluences), or a nanojet with a mesoparticle atop on a nanobump with 10-nm-thick walls, as a hemispherical cupola of the thinned film (lower fluences). Such nanojets with mesoparticles atop can be fabricated only by laser-assisted techniques. In this case, the fluence of the first laser pulse can be used to control diameters of such nanobump and microhole. Each type of the fabricated nanostructures corresponds to a specific range of the peak fluence: $F_{\text{hole}} > 0.3\,\text{J/cm}^2$ for microhole and $F_{\text{bump}} \approx 0.2$–$0.3\,\text{J/cm}^2$ for nanobump [15]. These two main types of laser-induced nanofeatures are considered here as efficient scatterers for the second spatially shifted fs-laser pulse, providing excitation of converging or diverging SPP waves (SPP focusing or defocusing) on the film surface.

Figure 1(a) shows double-pulse ablation region on the Au film surface: the first series of pulses fabricated the nanojets with the surrounding nanobump at $F \approx 0.25\,\text{J/cm}^2$, while the second series spatially shifted along x at $\approx 2\,\mu\text{m}$ imprinted the diffraction gratings, resulting from the interference of the second incident pulses and SPPs excited from the nanobump edges. As in the previous cases, the grating periods are approximately $\Lambda \approx 0.50 \pm 0.01\,\mu\text{m}$. Importantly, the second pulse does not only imprint the grating, but also destructs the Au nanobump, leaving the resulting nanojet to stand alone on the Si substrate. Apparently, such grating formation with the surface height modulation $\sim 30\,\text{nm}$ is caused by the Au film delamination from the silicon surface in the interference maxima, rather than film ablation.

In the second case, numerical simulation of the interference field on the Au film surface around the nanobump irradiated by the Gaussian beam shifted by $\approx 2\,\mu\text{m}$ along x-axis from the nanojet center (Fig. 1(b)) demonstrates at least 6 pronounced interference maxima with the period of $0.48\,\mu\text{m}$ (Fig. 1(c)). As seen, in these maxima, the peak fluence exceeds the nanobump formation threshold $F_{\text{bump}} \approx 0.2\,\text{J/cm}^2$. Therefore, such interference model for the grating formation is in excellent agreement with observed experiment results and allows to control its main parameters (height and the number of ridges) [16].

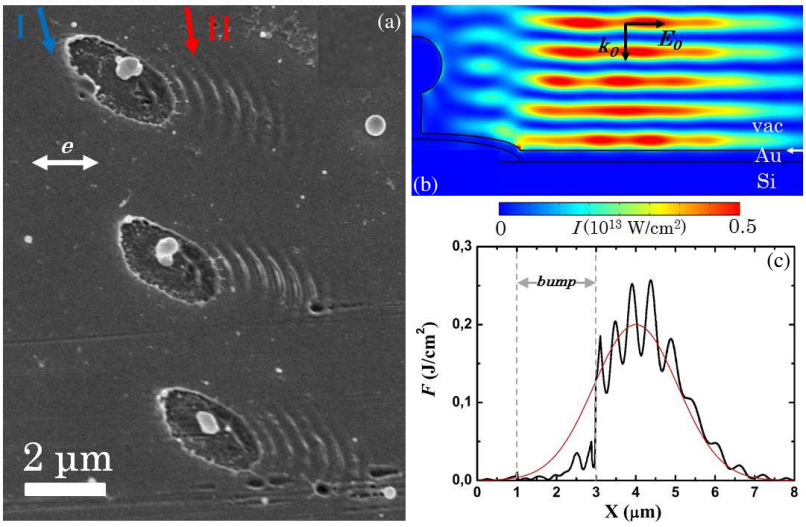

Figure 1: (a) SEM image of the Au film irradiated by the first femtosecond pulses at the peak fluence $F \approx 0.3\,\text{J/cm}^2$ along the direction marked by the arrow (I) and then by the second pulses at $F \approx 0.25\,\text{J/cm}^2$, spatially shifted along x-axis by the distance of $2\,\mu\text{m}$ (direction II). All SEM images were obtained at 45°-tilt. The white arrows indicate the polarization direction; (b) two-dimensional intensity maps calculated at normal incidence of the Gaussian beam near the edge of the nanobumps surrounding the nanojet; (c) fluence distribution near the Au film surface calculated for the second-pulse spatial shift $2\,\mu\text{m}$ (black curve) from the center of the nanobump surrounded the nanojet and in the case of smooth Au surface irradiation in the absence of the nanobump (red curve).

3. NANOANTENNA FABRICATION DUE TO FLASH-IMPRINT OF INTENSE FOCUSED SPP

100 fs, 744 nm linearly polarized Ti:sapphire laser pulses with a maximum pulse energy of 6 mJ in the TEM00-mode were focused by a silica lens (focal distance of 11 cm) onto a 4 mm-thick aluminum sample mounted vertically on an motorized translation stage. The mechanically polished and ultrasonically cleaned sample was located several mm above the focal plane to obtain a large spot diameter $D_{1/e} \approx 180\,\mu$m. The nanostructured sample surfaces were characterized using field-emission scanning electron microscopy (FE-SEM).

Nanoantenna fabrication on an aluminum surface was performed by two fs-laser pulses at the same peak fluence $F \approx 0.85\,\mathrm{J/cm^2}$ (slightly below the spallative ablation threshold $F_{\mathrm{spal}} \approx 0.7\,\mathrm{J/cm^2}$ [17]), following with a delay of a few seconds between them [11, 12]. After the first laser pulse an irregular array of round spallative pits with a surface density $\sim 10^7\,\mathrm{cm^{-2}}$ appeared on the surface (Figure 1(a)) at local fluences $F > F_{\mathrm{spal}}$ along an outer border of a macroscopic spallation crater. Their edges have widths of about $\Delta \sim 100$ nm, their bottom is semispherical appearing, in average, 100 nm below the initial surfacelevel (Figure 2). The average diameter of the pits depends on local laser fluence, but usually amounts to 1.3 μm. They result from intense sub-surface nanovoid generation (homogeneous nucleation) in the melted surface layer [18] at fs-laser fluences slightly lower than the spallation threshold Fs. Such pits with prominent edges respond to EM fields in the optical range as plasmonicnanolenses [19], providing excitation and sub-diffraction focusing of SPPs in their centers. The focusing in plasmonic lenses exposed by fs-laser pulses at $F \approx 0.85\,\mathrm{J/cm^2}$ results within each pit in the formation of a single nanojet (Figure 1), related to material expulsion and its ultrafast cooling [11, 12] expected for much higher fs-laser fluences, exceeding the threshold $F_{\mathrm{frag}} \approx 1.4\,\mathrm{J/cm^{-2}}$ for supercritical hydrodynamic (fragmentation) ablation [17].

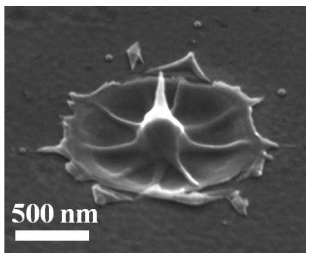

Figure 2: SEM image of aluminim surface with nanojet within microcrater formed under two femtosecond laser pulses irradiation.

4. CONCLUSION

The proposed new principle of all-laser nanoantenna fabrication is very simple and high-productive, but the physics beyond them is quite interesting and complicated. Both of the proposed methods induce a sequence of electrodynamic (surface plasmon-polariton [SPP] excitation and interference), thermal (melting, cavitation, ablation and ultrafast cooling), and hydrodynamic processes. In particular, SPP excitation leads to local energy deposition into a single sub-diffractive spot or into sub-wavelength periodical lines, while the thermal and hydrodynamic processes are important for nanoantenna formation.

ACKNOWLEDGMENT

This work was partly financially supported by the Government of the Russian Federation (Grant 074-U01) through ITMO Post-Doctoral Fellowship and President Scholarship (SP-2015).

REFERENCES

1. Fan, M., G. F. Andrade, and A. G. Brolo, *Anal. Chim. Acta*, Vol. 693, 7, 2011.
2. Knight, M. W., H. Sobhani, P. Nordlander, and N. J. Halas, *Science*, Vol. 332, 702, 2011.
3. Nakata, Y., N. Miyanaga, K. Momoo, and T. Hiromoto, *Appl. Surf. Sci.*, Vol. 274, 27, 2013.
4. Reininghaus, M., D. Wortmann, Z. Cao, J. M. Hoffmann, and T. Taubner, *Opt. Express*, Vol. 21, 32176, 2013.
5. Chen, L., T. Zhai, X. Zhang, C. Unger, J. Koch, B. N. Chichkov, and P. J. Klar, *Nanotechnology*, Vol. 25, 265302, 2014.

6. Kulchin, Y. N., O. B. Vitrik, A. A. Kuchmizhak, A. V. Nepomnyashchii, A. G. Savchuk, A. A. Ionin, and S. V. Makarov, *Opt. Lett.*, Vol. 38, 1452, 2013.
7. Kuchmizhak, A. A., Y. N. Kulchin, O. B. Vitrik, A. G. Savchuk, S. V. Makarov, S. I. Kudryashov, and A. A. Ionin, *Opt. Commun.*, Vol. 308, 125, 2013.
8. Zywietz, U., A. B. Evlyukhin, C. Reinhardt, and B. N. Chichkov, *Nat. Commun.*, Vol. 5, 3402, 2014.
9. Unger, C., J. Koch, L. Overmeyer, and B. N. Chichkov, *Opt. Express*, Vol. 20, 24864, 2012.
10. Emel'yanov, V. I., D. A. Zayarniy, A. A. Ionin, I. V. Kiseleva, S. I. Kudryashov, S. V. Makarov, and A. A. Rudenko, *J. Exp. Theor. Phys. Lett.*, Vol. 99, 518, 2014.
11. Gubko, M. A., A. A. Ionin, S. I. Kudryashov, S. V. Makarov, A. A. Rudenko, L. V. Seleznev, and D. V. Sinitsyn, *J. Exp. Theor. Phys. Lett.*, Vol. 97, 599, 2013.
12. Gubko, M. A., W. Husinsky, A. A. Ionin, S. I. Kudryashov, S. V. Makarov, C. R. Nathala, and I. V. Treshin, *Laser Phys. Lett.*, Vol. 11, 065301, 2014.
13. Lezec, H. J., A. Degiron, E. Devaux, R. A. Linke, L. Martin-Moreno, F. J. Garcia-Vidal, and T. W. Ebbesen, *Science*, Vol. 297, 820, 2002.
14. Liu, J. M., *Opt. Lett.*, Vol. 7, 196, 1982.
15. Kulchin, Y. N., O. B. Vitrik, A. A. Kuchmizhak, A. G. Savchuk, A. A. Nepomnyashchii, P. A. Danilov, and A. A. Samokhin, *Sov. Phys. JETP*, Vol. 119, 15, 2014.
16. Kuchmizhak, A. A., A. A. Ionin, S. I. Kudryashov, S. V. Makarov, A. A. Rudenko, Y. N. Kulchin, and T. V. Efimov, "Flash-imprinting of intense femtosecond surface plasmons for advanced nanoantenna fabrication," *Optics Letters*, Vol. 40, No. 8, 1687–1690, 2015.
17. Ionin, A. A., S. I. Kudryashov, S. V. Makarov, L. V. Seleznev, and D. V. Sinitsyn, *JETP Lett.*, Vol. 94, 34, 2011.
18. Leveugle, E., D. S. Ivanov, and L. V. Zhigilei, *Appl. Phys. A*, Vol. 79, 1643, 2004.
19. Liu, Z., J. M. Steele, W. Srituravanich, Y. Pikus, C. Sun, and X. Zhang, *Nano Lett.*, Vol. 5, 91726, 2005.